Statistical Analyses of Pore Radii on the Performance of PET-nanocomposite Membranes in the Removal of Iron and Anions F Rom Ibeshe River

Oluranti Agboola (funmi2406@gmail.com)
Covenant University https://orcid.org/0000-0003-4951-972X
Ajibola Ademola Khalih
Covenant University COE: Covenant University College of Engineering
Olagoke Oladokun
Covenant University
Augustine Omoniyi Ayeni
Covenant University
Frederick Uzokwe Chukwudubem
Covenant University
Olayemi Odunlami
Covenant University
Francis Elehinafe
Covenant University
Abdulrazaq Yahaya
Kogi State University
Lucey Moropeng
Tshwane University of Technology

Research Article

Keywords: PET-nanocomposite membranes, ImageJ, SEM, Pore radius, Python

Posted Date: May 11th, 2022

DOI: https://doi.org/10.21203/rs.3.rs-1596840/v1

STATISTICAL ANALYSES OF PORE RADII ON THE PERFORMANCE OF PET-NANOCOMPOSITE MEMBRANES IN THE REMOVAL OF IRON AND ANIONS FROM IBESHE RIVER

Oluranti Agboola[1*], Ajibola Ademola Khalih[1], Olagoke Oladokun[1], Augustine Omoniyi Ayeni[1], Frederick Uzokwe Chukwudubem[1], Olayemi Odunlami[1], Francis Elehinafe[1], Abdulrazaq Yahaya[2], Ojo Sunday Isaac Fayomi[3], Lucey Moropeng[4]

[1]Department of Chemical Engineering, Covenant University, Ota, Nigeria
[2]Department of Pure and Industrial Chemistry, Kogi State University
[3]Department of Mechanical and Biomedical Engineering, Bells University of Technology, Ota, Ogun State, Nigeria
[4] Department of Chemical, Metallurgical and Materials Engineering, Tshwane University of Technology, South Africa
*Corresponding: Authors Email: funmi2406@gmail.com

Abstract

Ibese watershed has been experiencing lower water quality due to industrialization. Polyethylene terephthalate (PET)-graphene oxide (GO) nanocomposite membranes (M1, M2 and M3) synthesized by non-solvent-induced phase separation on polyester nonwoven support using polyethylene glycol (PEG) as additive was reported. The membranes (M1, M2 and M3) were respectively synthesized with 1wt%, 2wt% and 3wt% GO. The morphology of the membranes was characterized by scanning electron microscopy (SEM). ImageJ software was used to study the pore size distribution of the membranes. Python was use for the statistical study using the uniform distribution curve and mean and the results show that the radius data distribution is tightly clustered around the mean. The adsorption performance of composite membranes was examined for the removal of ions from the river water. The membranes were assessed through flux, adsorption capacity and the rejection of iron and anions found in Ibese river water. M3 membrane gave higher rejection rate for the three anions and iron. The % rejection of nitrate ion with M3 membrane is 96%, 85%%, 72% and 60% respectively for NO^{3-}, Cl^{-}, HCO^{3-} and Fe. Increase in the quantity of GO increased water flux and the maximum water flux was attained with 3wt% GO.

Keywords: PET-nanocomposite membranes, ImageJ, SEM, Pore radius, Python

Introduction

Water makes up 60% of the human body and is vital to all life on Earth. 97.5% of the water on the planet's surface is salty, which cannot be utilized directly since 80% of this saltwater is

frozen in the icecaps or mixed as soil moisture. Freshwater accounts for the remaining 2.5%, which is believed to be adequate to support all life on Earth. Unfortunately, this water is not evenly distributed globally and is not accessible in abundant quantities when and where it is needed. Most of the available water is heavily polluted by agricultural and industrial waste and cannot be consumed, so the key issues that need to be addressed are water quality and quantity [1].

One of the most important environmental challenges is the contamination of rivers, streams, and wetlands with toxins. There is a great deal of damage caused by waterborne chemical waste entering rivers, streams, and ponds. As rain falls and penetrates the rock, it usually dissolves some of the iron at varying concentrations. The rain transports the iron along with it as it continually penetrates through the rock and soil. With time, this rainwater moves into groundwater or goes into sources of freshwater such as lakes and rivers; which could come to be part of the local water supply. Municipal water systems that get their water from these sources could culminate into high levels of iron in their water, and the filters used by the Municipal to remove bacteria and other detrimental contaminants might not always filter it out. In addition to that, wells that take water from aquifers with iron content might also contain high concentrations of iron. Generally, iron in water is of one of two forms; ferrous iron, which is soluble in water, and ferric iron, which is insoluble in water. Typically, water that contains ferrous iron is visually faint from pure water owing to the fact that the iron is evenly dissolves in the water; hence, the water will remain clear. However, when the water eventually gets to a home pressure tank (well tank) or pours out into the air, the iron will be oxidized and turns into the insoluble ferric iron. As a result, the iron will then be visible and starts to affect water quality [2]. Present, the recommended limit for iron in water is 0.3 mg/l (ppm). This is centred on the appearance and taste rather than on any detrimental health effect [3]. In addition to iron, there are different anions in river water.

Wastewater from all over; rain, households, industries, non-domestic sources, groundwater along the Abuja axis in Ikorodu all flow to the same place, Ibeshe River. Ibeshe River water contains iron which has deteriorated the river water beyond acceptable levels due to uncontrolled discharge of rain water, untreated wastewater and solid debris into the river. The development and industrialisation of Ikorodu's Ibese watershed also contributed to the low quality of water, affecting the aquatic ecosystem and downstream users. This has increased the scarcity of water in that area of Lagos, in spite of its proximity to water, Lagos has limited access. Currently, the city’s water demand per day is greatly beyond the production by the

municipal utility Lagos Water Corporation. In addition, the utility does not even provide half of the needed amount of water per day; which is 540 million gallons, leaving Lagos with an enormous water shortage of about 320 million gallons [4].

There are numerous ways of treating wastewater, many techniques for wastewater treatment have been developed; such methods include reverse osmosis [5], ion exchange [6], gravity [7] and adsorption, among others. As a result of its cheap cost and flexibility, adsorption is widely utilized to remove contaminants from water. Adsorbents of various types, such as polymer nano-composites, activated carbon, and magnetic nanoparticles, may be used in the treatment of wastewater. They may assist in the removal of harmful pollutants such as heavy metals, even when used in little amounts. Despite the fact that adsorption can remove the vast majority of pollutants from water, it is subject to a number of limitations, including a scarcity of suitable adsorbents with high adsorption capacity and a ban on their commercial usage [8]. This is why more effective methods such as membrane technology are required.

Nanocomposite membranes are considered collections of innovative filtration materials that is made of nanofillers dispersed a polymeric or inorganic oxide matrix prior to casting functionalizes them. The modification of nanocomposite membranes is considered advanced membranes technology because it enhances the treatment of water and wastewater as a result of the properties of nanomaterials embedded in the membranes. The integration of nanofillers usually changes the membrane properties by improving its separation performance, improve its pore structure and permeability, stabilize flux, and it gives the impression of an anti-fouling behaviour [9, 10]. Particles contained the fluid interrelate with the membranes physically or chemically for all filtration modes, resulting in membrane fouling, which is the process in which foulants being deposited on the surface of the membrane or within the pores. Membrane fouling occurs via three principal mechanisms: (1) adsorption, which is a mass deposit process in which small particles stick to the pore walls and then shrink the pore effective radius; (2) blocking, which is a discrete process in which particles that are larger than pores partially or completely cover the entrance of a pore; and (3) caking, is the process in which an added stratum of porous medium, consists of the particles transported by the flow, forms on top of the membrane surface towards the end of filtration [11].

The dispersion of nanofillers in membranes to form nanocomposites used for membrane separation processes not only improve membranes properties, it also magnifies the technology possibilities of treating different kinds of wastewater. Different types of nanoparticles have

been used to enhance membrane performance; however, literature has recently documented that inorganic nanoparticles could have the capability of being utilized as fillers for the enhancement of microporous ultrafiltration (UF) membranes properties [12-14]. The properties that are envisage to be enhanced are water permeability, mechanical and thermal properties together with fouling propensity, in as much as the quantity of nanoparticles dispersed in the polymer was not in excess. Titanium dioxide (TiO_2) nanoparticle is among the most studied inorganic nanoparticles utilized for the preparation of nanocomposite membranes [15]. Another inorganic nanoparticle that is most studied is graphene oxide (GO) nanoparticle. The utilization of graphene oxide for synthesizing nanocomposite membranes could be designed in two ways [16]. The first way is the direct employment of graphene oxide as a separating stratum [17, 18] while the second one is the integration of graphene oxide in polymer matrix for the enhancement of the membrane performance [19]. Apart from the methods of integrating graphene oxide in membranes; there are also different methods of synthesizing graphene oxides, these methods also have effects on membranes performance. Sali et al. [20] studied the influence of GO synthesis methods on features and performance of polysulfone-graphene oxide mixed matrix membranes for the removal of oil from an oil-water emulsion. The GO used in their study was synthesized through the Hummers', Tour, and Staudenmaier methods. Their study showed that GO synthesized via the Staudenmaier method exhibited a higher concentration of the more polar carbonyl group, which resulted in the upsurge of the membrane hydrophilicity and porosity compared to GO synthesized via the Hummers' and Tour methods. Conversely, the GO synthesized via Hummers' and Tour methods exhibited larger sheet size, and they are more effective in improving the mechanical properties of the polysulfone membrane.

In addition, researchers recently focused on the utilization of polymer materials that are cost-effective as an alternative polymer for the preparation of membranes. The notion of employing waste as a precursor for the fabrication of membranes have the capacity to assist in curbing the disposal of waste to our environment while offering a smart, low-cost means of utilizing fossil-based polymers as membrane material [21]. Furthermore, substitutes to conventional polymers resulting from fossil fuels are desired, as the processing of fossil-based polymers is associated to fossil resource depletion and it is also connected to human toxicity, marine eco-toxicity, and global warming as a result of the volatile emission [22, 23]. With regards to these threats, there has been increasing research interest in employing polymers derived from waste (like chitosan, cellulose, keratin and rubber) as substitutes for synthesizing membranes.

The main focus of this investigation is to study the impact of pore size variations the ensued from the synthesis of Polyethylene terephthalate-graphene oxide nanocomposite membranes in evaluating their performance in terms of flux and rejection for the removal pollutants such as iron and anions from Ibese river. In order to enhance the size of the GO nanoparticle, a modified Hummer's method [24] would be used for the GO synthesis. Literature also documeted that larger nanoparticles sometimes adhered to the exterior of the membrane which will caused minimal disruption. It is hence envisaged that GO produced by a modified Hummer's method would enhance the pore size of the membranes [25]. The nanocomposite membranes would therefore be characterized by using SEM to study the pore size distribution and morphology of the membranes.

Materials and Method

PET Material

Polyethylene terephthalate (PET) was obtained from waste plastic bottles. Polyethylene glycol (PEG-600), dichloromethane (DCM), trifluoroacetic acid (TFA), graphite powder, Hydrochloric acid (HCL), phosphoric acid (H_3PO_4), Sulfuric acid (H_2SO_4), potassium permanganate (KM_nO_4) are reagents and chemical used for this study. They are analytical grade reagents and gotten from Sigma-Aldrich.

Graphene Oxide Synthesis

Graphene oxide was synthesized from pure graphite powder of 20 µm by employing a modified Hummer's method [24]. A 9:1 ratio of sulfuric acid (H_2SO_4) to phosphoric acid (H_3PO_4) was used; the solution was then mixed with 0.225 g graphite powder. 1.32 g potassium permanganate was then gradually added (in dropwise) to the solution ($KMnO_4$) and subjected to 6 hours agitation using stirrer. After 6 hours of agitation, 1 mL hydrogen peroxide (H_2O_2) was progressively added and stirred for 10 minutes to eliminate excess $KMnO_4$. Exothermic reaction occurred and subsequently cooled. The solution was centrifuge for 7 minutes of at 5000 rpm using an Eppendorf Centrifuge 5430R, 10 mL of HCl and 30 mL of distilled water were added. The supernatant was then decanted away and the residuals was rewashed trice with HCl and deionized water. A 6-hour bake at 125°C dried the washed GO solution, producing GO powder [24]. Fig. 1 depicted the synthesized GO oxide from graphite powder.

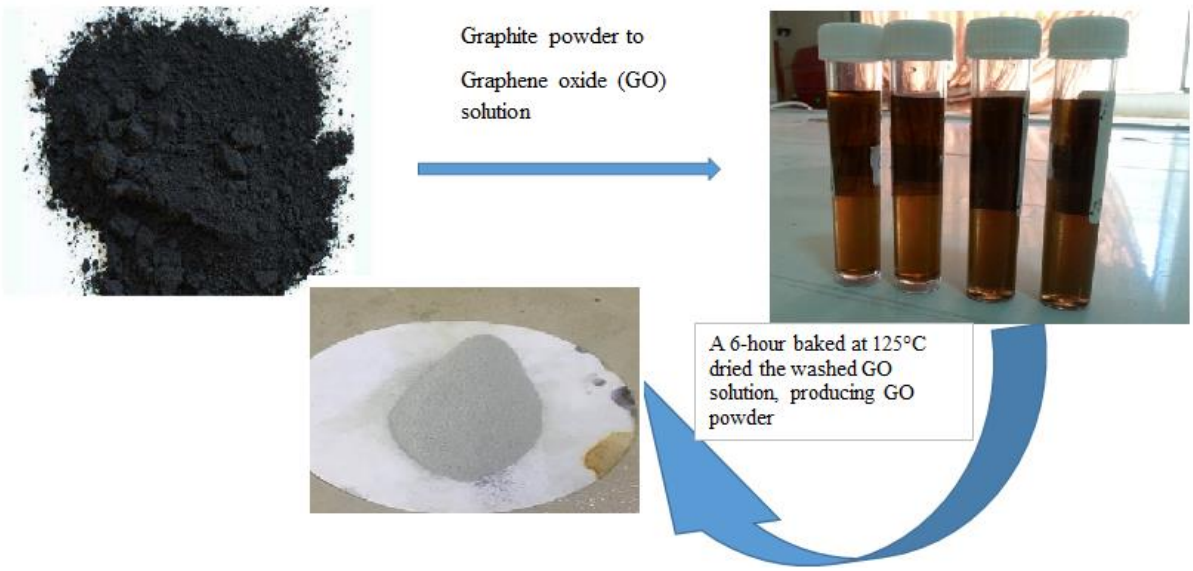

Fig. 1 Pictorial representation of synthesized GO oxide from graphite powder. The GO powder was doped in the PET to synthesize the nanocomposite membrane.

Preparation of PET

The PET bottles were first melted to molten and then crushed into sizable bits using electrical crusher. The sizable bits of the PET were processed to powdery nano sizes using mechanical grinder. An industrial sieve shaker was used to sieve crushed material off the desired particle size (100 µm) and the remnant is crushed again to obtain the desired particle size.

Synthesis of PET-graphene oxide Nanocomposite Membrane

The casting solutions method was used in synthesizing the PET-graphene oxide nanocomposite membranes. 20 g of PET was dissolved in trifluoroacetic acid and dichloromethane in ratio 1:2 and the solution was stirred for 1 hour at room temperature (25 °C) with a magnetic stirrer until it became homogenous. In order to enhance the membrane's performance, polyethylene glycol was continuously added as additive in dropwise while stirring until the solution was fully clear and homogenous at around 90 minutes. The resulting polymer solutions were kept at room temperature without being stirred to eliminate trapped air bubbles in the casting solution [26]. The experimental design used for the preparation of the membranes is shown in Table 1.

Non-solvent-induced phase separation (NIPS) was used to produce all flat sheet membranes; a 15 cm by 20 cm glass plate was used to cast the membranes. This was accomplished by pouring the casting solution over a flat polyester nonwoven fabric set at room temperature on the casting plate and casted it using a casting knife. Immediately thereafter, a thin polymeric film

supported on a polyester nonwoven support was separated from the glass. The membranes were cleaned and stored in distilled water.

Table 1 Design of Experiment

SAMPLE	TFA/DCM (wt%)	PET (wt%)	PEG (wt%)	GO (wt%)
M1	72	20	10	1
M2	72	20	10	2
M3	72	20	10	3

Filtration Process Procedure and Mechanism

Fig. 2 displays the schematic representation of the membrane separation process unit that was used for this study. This unit contains a membrane cell with flow in, flow out and pressure pump. The synthesized nanocomposite membrane was placed inside the membrane cell. The water sample from Ibese river was fed into the membrane cell through the pump with a control panel that was used to control the flow rate of water. The pump outlet hose was connected to the membrane cell inlet and the pump inlet hose was placed in the wastewater tank. The feed was allowed to stabilized for 20 minutes with all valves closed. The cell pressure pump spun around to upsurge water movement and are powered by a DC electric motor. At every 15 minutes time interval, the permeate was collected in a beaker by opening the valve at the bottom of the cell and the valve on the top side of the membrane cell was opened so as to collect the retentate. The schematic representation of the transport mechanism of the membrane filtration process is depicted in Fig. 3. The transport mechanism involves the use of a driving force (pressure pump) which forces the feed stream that flows perpendicularly to the membrane surface to move through the membrane. The components retained on the surface of the membrane will accumulate to form a layer of cake, which will result in the reduction of permeate as a result of added resistance to the filtration of the layer of cake [27].

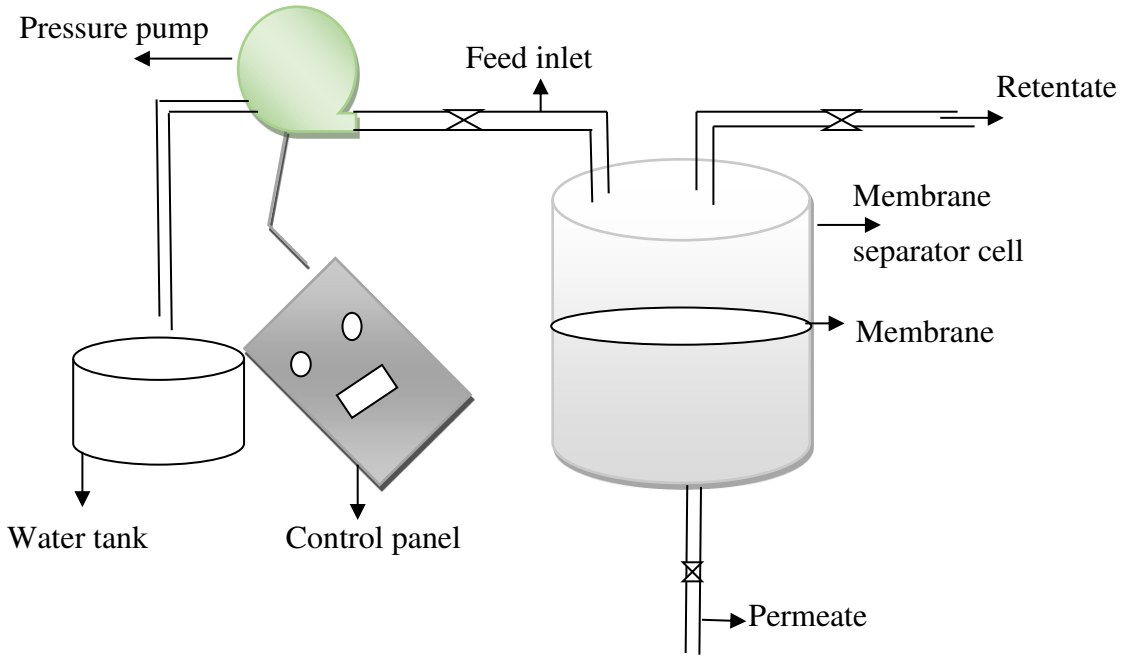

Fig. 2 Schematic representation of the membrane separation unit. The unit comprises of a membrane cell with flow in and flow out together with a pressure pump and attached to it, is the flow control panel.

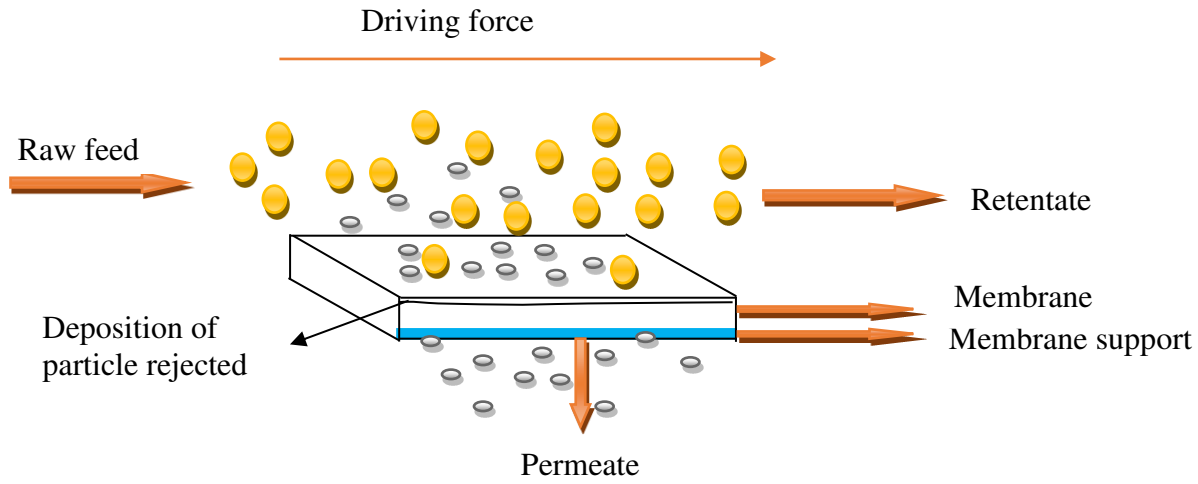

Fig. 3 Schematic representation of the membrane filtration transport mechanism (Modified from [28]

Brunauer-Emmett-Teller (BET)

Any carbon materials can be well analysed knowing the BET surface area as determined by utilizing the analysis of nitrogen adsorption isotherms. BET was used to explain the physical adsorption of gas molecules on the GO surface.

Scanning Electron Microscopy (SEM) / Energy Dispersive X-Ray (EDX)

The morphological structure of the synthesized PET-graphene oxide nanocomposite membranes was examined with the utilization of scanning electron microscopy. It is a tool commonly used for showing the microstructure of a membrane material [29]. The morphological analysis of the membranes was attained by employing a fast-tracking voltage of 15 kV, operating with a low beam mode for preventing the samples from been damaged. The samples prepared were firmly fit in the specimen chamber of the microscope, coated with a platinum coating of electrically conducting material via the deposition of the coating material on the sample employing a low vacuum sputter or high vacuum evaporation.

Theory

ImageJ is a Java-based image processing program technologically developed at the National Institutes of Health and the Laboratory for Optical and Computational Instrumentation. It is an open source software that facilitates the processing and analysis of scientific images. For the purpose of this work, the average pore size distribution was studied using ImageJ Software.

Python software was used to statistically analysed the data extracted from ImageJ. The pore radius extracted from ImageJ was analysed using Quartiles analysis using a NumPy. It is part of descriptive statistics that gives a better understanding of the data at hand. Quartiles analysis was used to understand the central tendency which is a solitary value that makes an effort to pronounce a set of data by detecting the central position contained within the set of data. Then, this analysis should have the capacity of predicting precise porosity of membrane microstructures for diverse sets of input parameters. Through the variation of pore sizes and the number of sites (n) can be located. Additional input variable that can be used to analyze pores of membrane from the structural morphology is the radius r.

The microstructure generated will be capable of adjustment in order to analyze quantified overall porosity together with any locally targeted porosity (which can be termed a porosity distribution function). This is attainable through the utilization of a Gaussian filter distribution. On the premise that the Gaussian filter is separable and could be utilized for every successful spatial direction; this study then utilized the logarithms to process pore radii as a replacement of the radii themselves and it was given for 1-D Gaussian as equation 1 [30]. The parameters of the Gaussian filter distribution were determined based on the grouped quartiles analysis.

$$N(\mu,\sigma^2)=\frac{1}{\sigma\sqrt{2\pi}}e^{-\frac{(x-\mu)}{2\sigma^2}} \quad (1)$$

The cumulative distribution function for a function with normal distribution is given as:

$$\phi(x)=\frac{1}{2}\left(1+erf\left(\frac{x-\mu}{\sigma\sqrt{2}}\right)\right) \quad (2)$$

Where erf is the error function

$$erf(z)=\frac{2}{\sqrt{\pi}}\int_0^2 e^{-x^2}dx \quad (3)$$

X = normal random variable, i.e., X~N (μ, σ^2)

Where *x* represents the distance from the observed center point, σ (sigma) represents the standard deviation of the pore radius population and μ represents the population mean of the normal distribution.

Permeation, Rejection and Adsorption Study

The permeate flux and rejection of iron and anions together with adsorption were studied as a function of time. The observed rejection, which is the measure of how well a membrane retains a solute, was calculated by Equation 4. While the permeate flux Jv (L/m^2 /hr) was studied by taking the measurement of the volume of permeate collected in a given time interval divided by the membrane area (A) by using Equation 5. The temperature of the flux was normalized by temperature correction factors.

$$\%\,\mathrm{Re}\,jection=\left(1-\frac{C_p}{C_i}\right)\times 100 \quad (4)$$

$$J_v=\frac{Q}{A} \quad (5)$$

In the isothermal adsorption study, all the anions and iron was study using their initial concentrations in the river water. The equilibrium adsorption capacity of the membranes was computed using equation 6.

$$Q_t=\frac{V(C_o-C_t)}{m} \quad (6)$$

Q_t in mg g^{-1} is the adsorption amount of the anions and cations at different time t, C_0 is the initial concentration in mgL^{-1} and C_t is the concentrations at time t, V (L) is the volume of the solution and m (g) is the mass of the membrane.

Results and Discussion

BET Surface Analysis of Synthesized GO and the Membranes

BET surface analysis is a very valuable measurement for surface area and porosity of many synthesized materials. The surface area to volume ratio of nanomaterial significantly contribute in the determination of properties of synthesized materials. The pore size distribution and the reactive surface area of the GO was analyzed by adsorption/desorption under N_2 in bath temperature of -195.750°C and ambient temperature of 22°C by BET measurement. The Brunauer-Emmett-Teller of GO surface area and pore size volume of GO are shown in Fig. 4. The total active specific surface area of GO is 332.850 m^2g^{-1}. The adsorption and desorption cumulative surface area of the pore was calculated by BJH method from nitrogen curve to be 17.000 Å. The cumulative pore volume of the GO is 0.453300 cm^3g^{-1} (Fig. 4b), respectively. The BET measurement further gave an adsorption and desorption average pore size as 32.4540 Å and 32.4544 Å respectively. The isotherm curve of GO depicted that in nature, the material is porous with a hysteresis loop at elevated partial pressure [31,32]. This can be confirmed from the surface area (332.850 m^2g^{-1}), as the graphene oxide exhibited high surface area owing to the presence of interconnected pores networks.

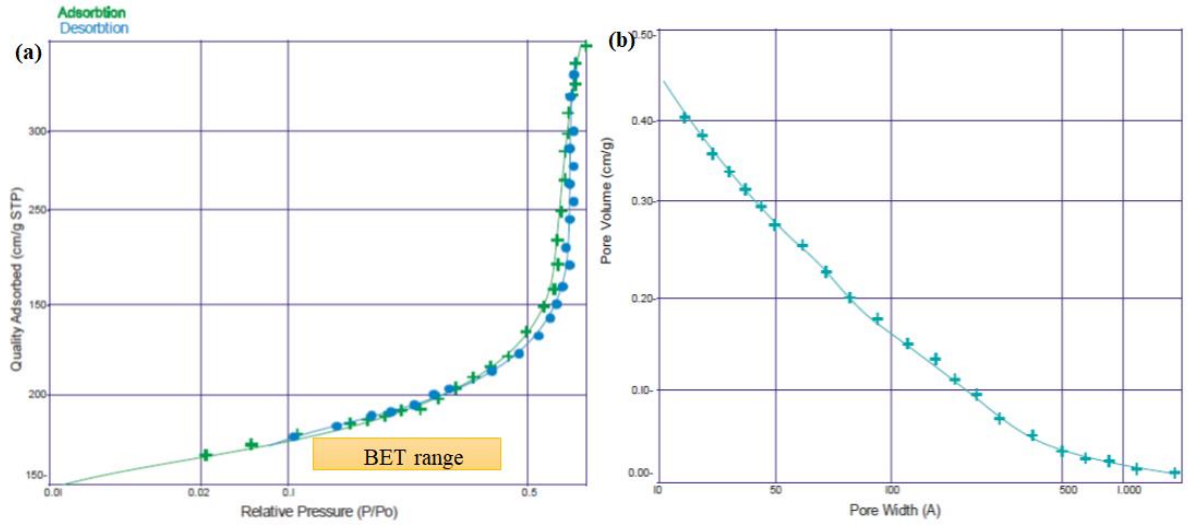

Fig. 4 Brunauer-Emmett-Teller of (a) Surface area of GO and (b) Pore size volume of GO.

SEM/EDX study

The morphological structure of the PET-graphene oxide nanocomposite membranes was analyzed using SEM. Fig. 5 show PET-graphene oxide nanocomposite membranes with (a) having GO 1wt. % incorporated in 20wt.% PET and 10wt.% PEG, (b) having GO 2wt. % incorporated in 20wt.% PET and 10wt.% PEG and (c) having GO 3wt. % incorporated in 20wt.% PET and 10wt.% PEG. There was really no acute difference between the membranes. However, the morphology of the three membranes has structure possessing inter-winning fibrous network with numerous pores and with Fig. 5c having some wrinkled morphology added to the inter-winning fibrous network. Thus, these membranes are highly symmetric porous membranes with rigid, highly voided with randomly distributed interconnected pores. Therefore, only molecules that are significantly variant in size would be separated efficiently by these membranes. In order to examine the quantity of elements of membranes, EDX was conducted. Fig. 6 depicts the EDX spectra of synthesized membranes and the alterations in the proportion of each element with respect with the amount of GO integrated into the membranes. From Fig. 6a, the 1wt. % GO incorporated in 20wt.% PET and 10wt.% PEG showed decrease atomic ratio of carbon and increase atomic ratio of sulphur. The atomic ratio carbon in the membranes increase with increasing amount of GO while the atomic ratio of sulphur reduces with increasing amount of GO (see Figs. 6a, 6b and 6c) [33]. In addition, the EDX spectrum of all the PET-graphene oxide nanocomposite membranes represents carbon and oxygen peaks at 0.23 and 0.52 keV. An elevated peak for carbon is observed as a result of the higher carbon content that was more than oxygen in PET-graphene oxide nanocomposite membranes. This is in accordance with the study of Jang et al. [34]. These results showed that GO exist in the synthesized PET-GO nanocomposite membranes.

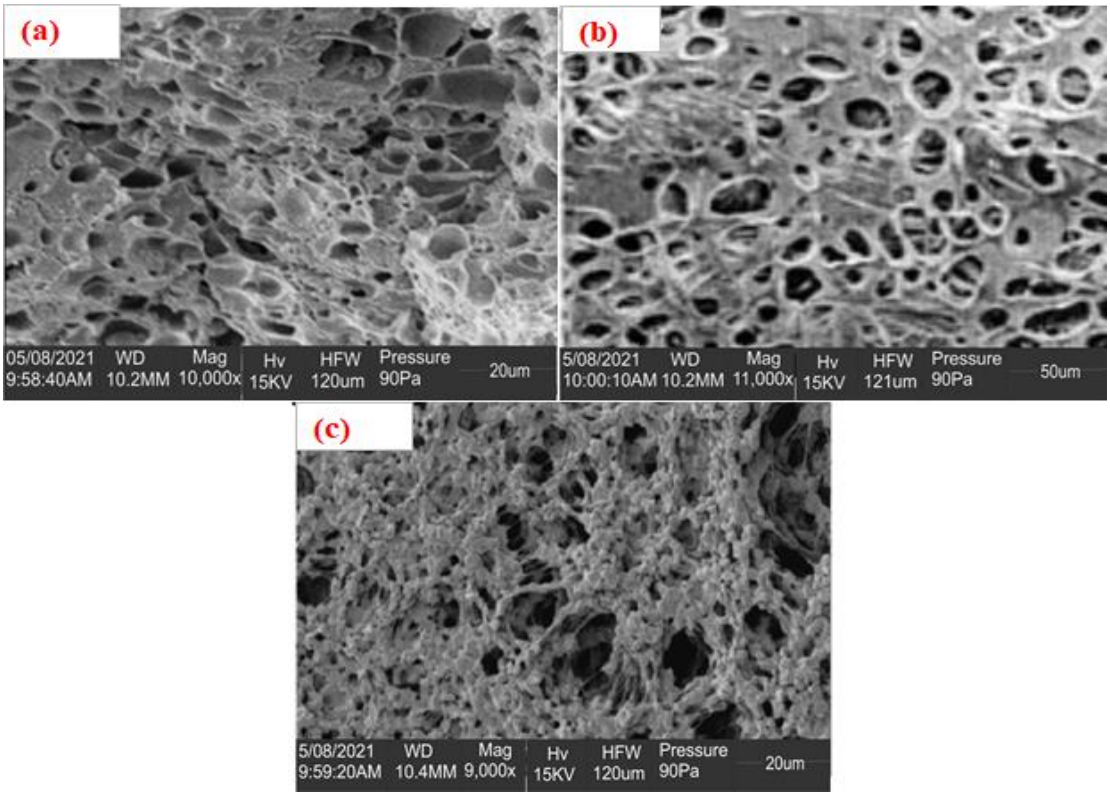

Fig. 5 SEM micrograph of PET-graphene oxide nanocomposite membranes; (a) - GO 1wt. %, (b) - GO 2wt. %, (c)-GO 3wt. %

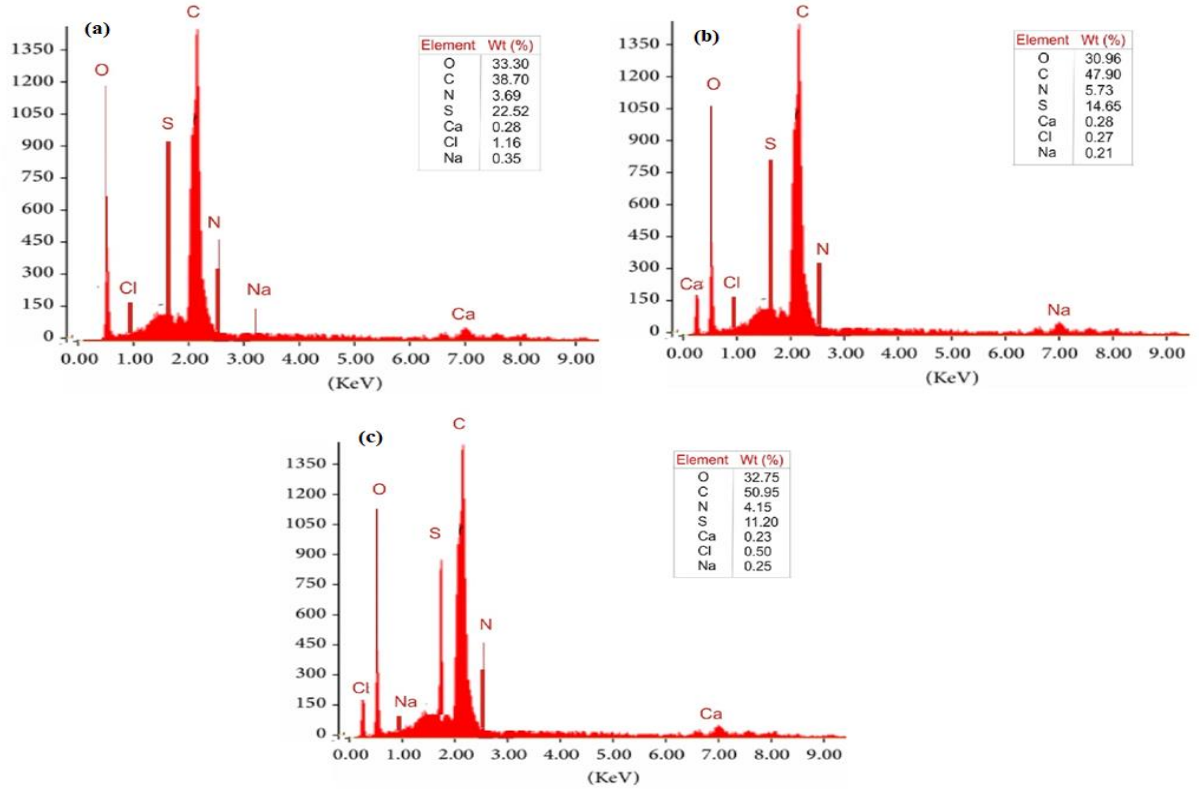

Fig. 6 EDX spectral of PET-graphene oxide nanocomposite membranes; (a) - GO 1wt. %, (b) - GO 2wt. %, (c)-GO 3wt. %

ImageJ Study

Fig. 7 depicts the pore size distribution of PET-graphene oxide membranes. It was observed that the number of pores decreases with increase in the quantity of GO embedded in the membranes. It was also observed that, the more the quantity of GO embedded in the membrane the smaller the sizes of the pores. The figure further shows that the pore size distribution varies; this is confirmed in Fig. 7. The pore sizes range from few micrometers to nearly 100 µm. The average pore sizes for M1, M2 and M3 respectively are 32 µm, 0.55 µm and 0.23 µm. In course of comparing the pore sizes of the membrane, Fig. 7 shows that increase in the quantity of GO embedded in the membrane leads to more distribution of pore size. Smaller quantity of GO (1wt%) results in more consistency in membrane pore size as the distribution is less [35].

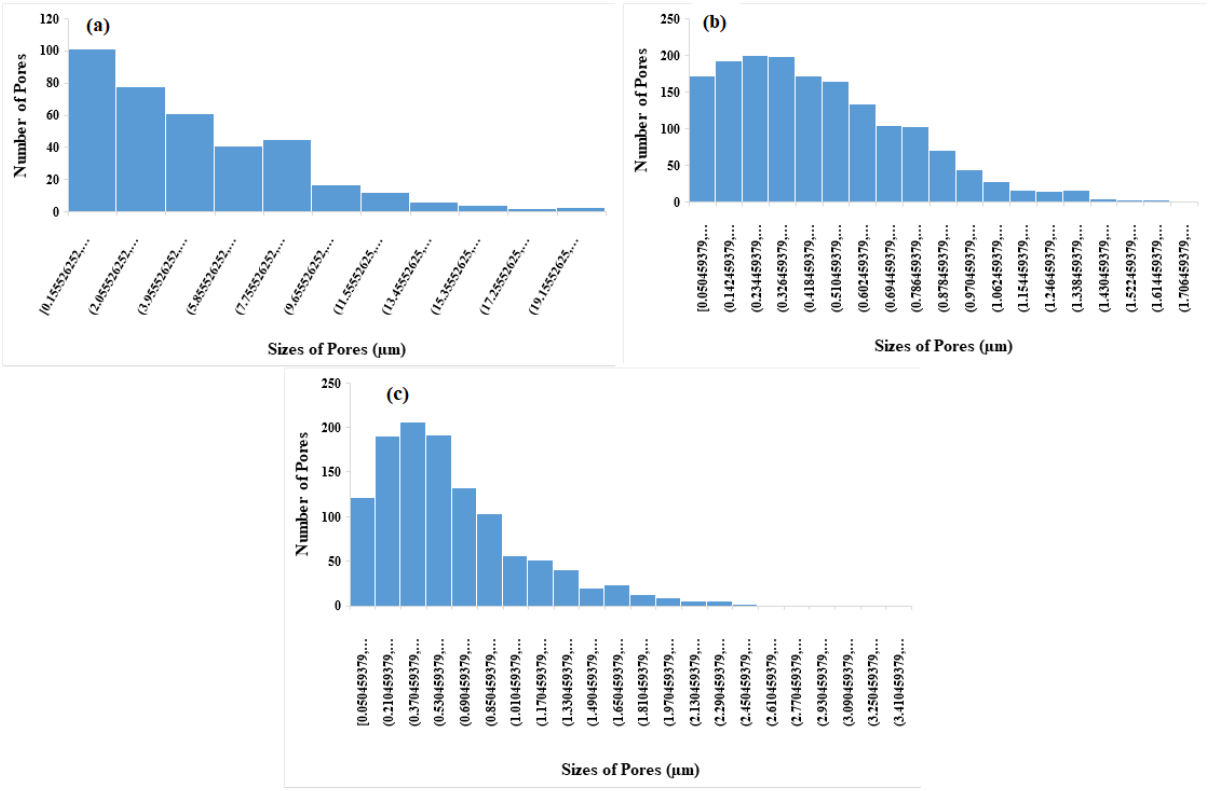

Fig. 7 Pore size distribution of PET-graphene oxide membranes (a) M1, (b) M2, (c) M3

Statistical Analyses

The features of membrane pore structures (pore size, pore size data distribution and pore density) ought to be the strength of the membrane industry because these features support the filtration properties of membranes. Fig. 8 shows the distribution of subsequent probabilities of M1, M2 and M3 with Quartiles analysis using a NumPy. The quantiles are the set of values that divides the radius dataset into groups of four equal size. This framework is useful to draw a

qualitative pore radius landscape, which will predict a minimum of radius size for the filtration. Beyond that radius size; however, still within an intermediate size in the quartiles, the pore seems to have a tendency to shrink towards the right, since the data distribution towards the dominates lower frequency. The areas with higher frequency for the three membranes serve as the critical radius that represents the active pore structure of the pore formation, which should be taken as the pore area for the membrane filtration.

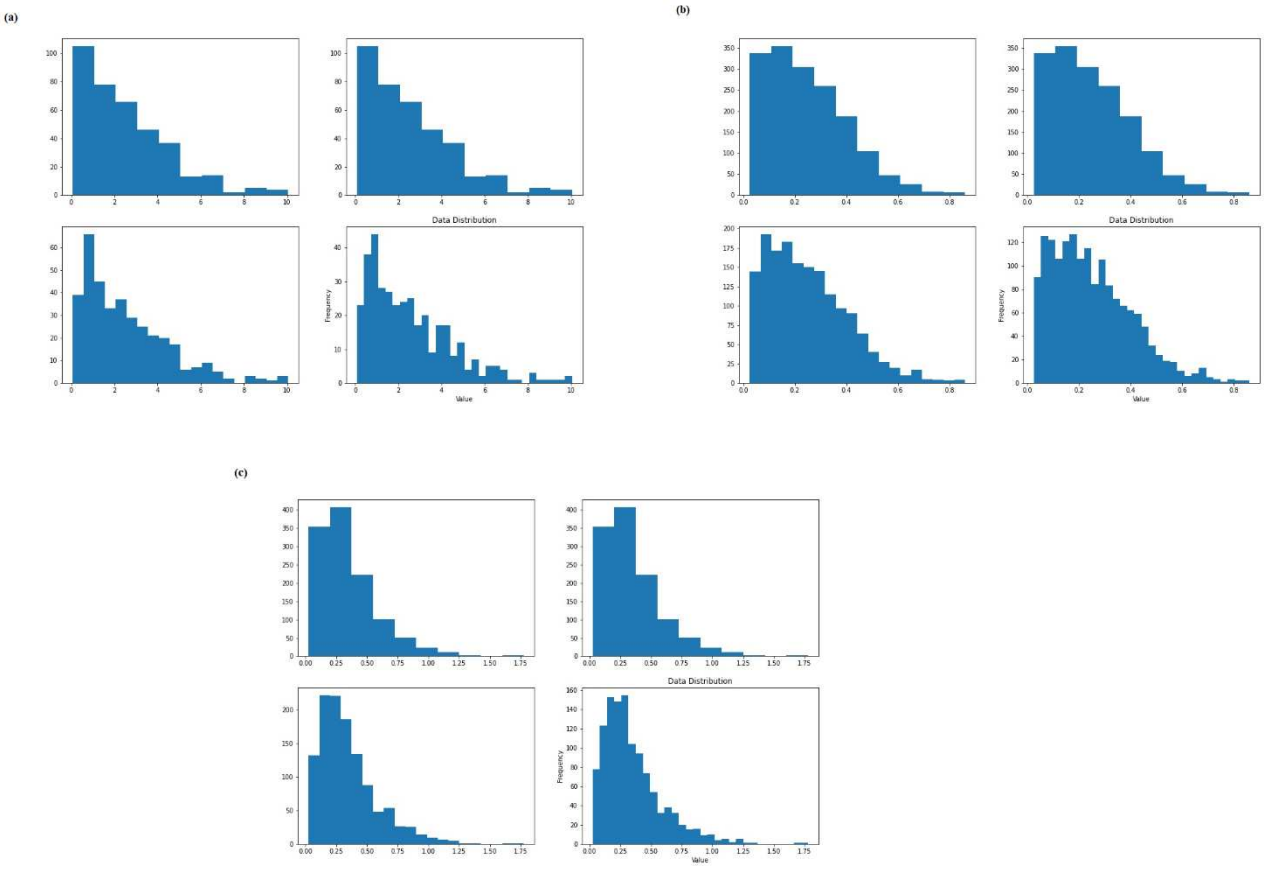

Fig. 8 Distribution of subsequent probabilities of M1 (a), M2 (b) and M3 (c) with Quartiles analysis using a NumPy

The statistical analyses were further done on the assumption the variable (pore radius) x is assumed to be uniformly distributed if the density function is:

$$f(x) = \frac{1}{a-b} \qquad (7)$$

For $-\infty < a \leq x \leq b < \infty$

The parameters of a standard uniform density are a = 0 and b = 1; hence, the probability density function for standard uniform density is expresses as:

$$f(x)=\begin{Bmatrix}1,0\le x\le 1\\0,otherwise\end{Bmatrix} \tag{8}$$

The data distribution of the membrane pores shown in Fig. 9 depicted that pore size distribution on the membranes is another factor that could have impact on the reliability of membrane separation. The data distribution is in conformity with Fig. 6 which depicted that upsurge in the quantity of GO integrated in the membrane resulted in more distribution of pore size. Smaller quantity of GO (1wt%) results in lesser distribution of data. However, it can be observed that the shape of the uniform distribution curve is rectangular for the three membranes. For a uniform distribution, a and b are the parameters.

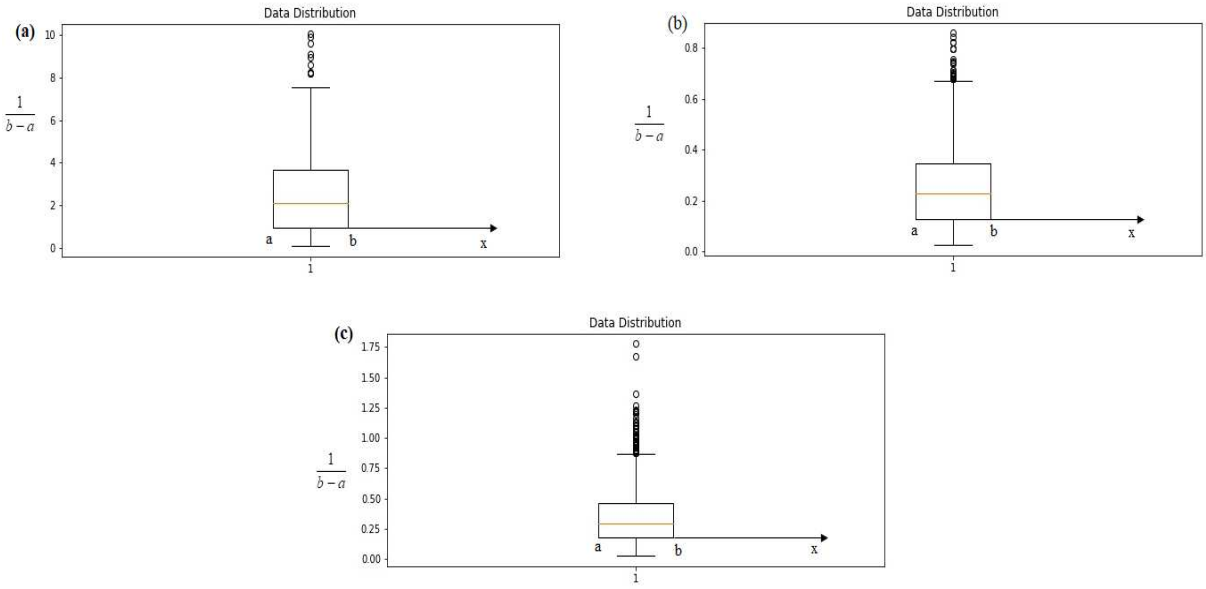

Fig. 9 The radius of pore distribution of PET-graphene oxide membranes (a) M1, (b) M2, (c) M3

Fig. 10 shows the distribution of mean of M1, M2 and M3 using the pore radii data via the central tendency. Central tendency infers the propensity of the data points to cluster around its central or middle-most value. The two most commonly used measures of central tendency are mean and median. Central tendency pronounces how far away the radius data points tend to fall from the centre. The Fig shows that the radius data distribution is tightly clustered around the mean with M1 having the of 2.5, M2 having the mean of 0.25 and M3 having the mean of 0.35. This shows that the more the graphene oxide imbedded in the membrane the lesser the value of the mean.

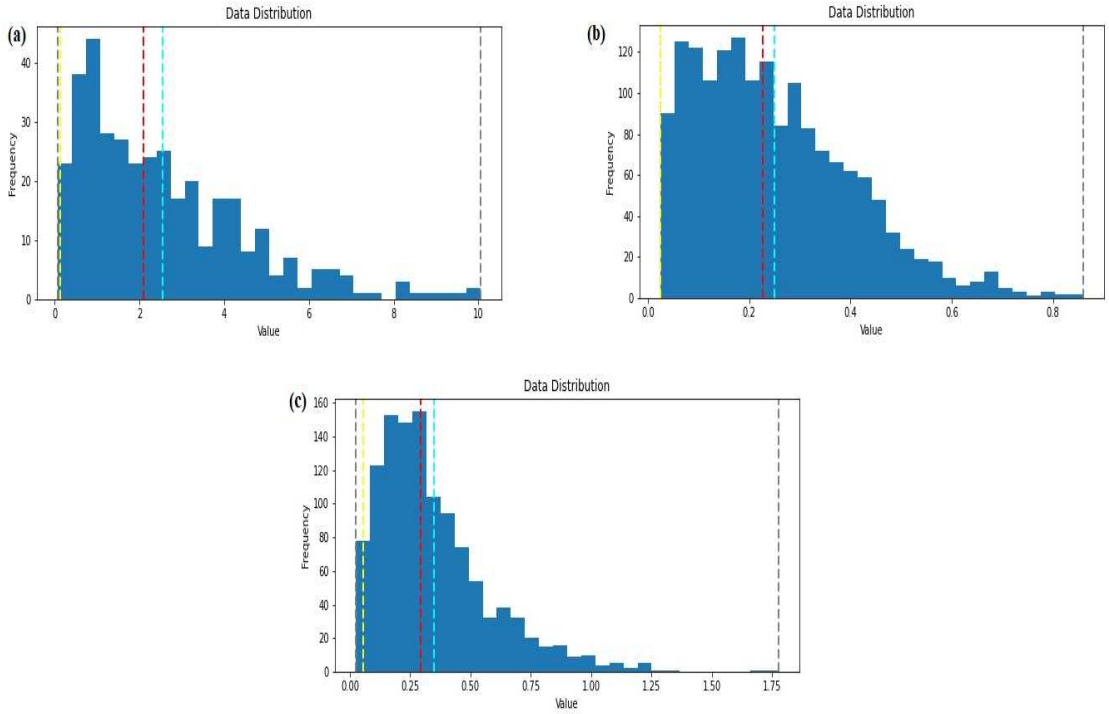

Fig. 10 The distribution of PET-graphene oxide membranes (a) M1, (b) M2, (c) M3, showing the mean and mode of pore radius

Fig. 11 shows the distribution of the membranes microstructures of the three membranes. The figure reflects the averages of microstructures with respect to aforementioned parameter (mean and pore radius). Hence, in order to analyze the impact of porosity on the membrane filtration, the averages of the microstructure for each porosity value specified in the microstructure generated were analyzed using the uniform distribution curve and mean. It shows that the porosity increases with increasing quantity of GO. As stated earlier, the mean and mode relate to the direct characteristics of the membrane microstructure. This is in good accordance with the pose size distribution depicted in Fig. 7. It is also evidently observed that the upsurge in porosity resulted in larger frequency values.

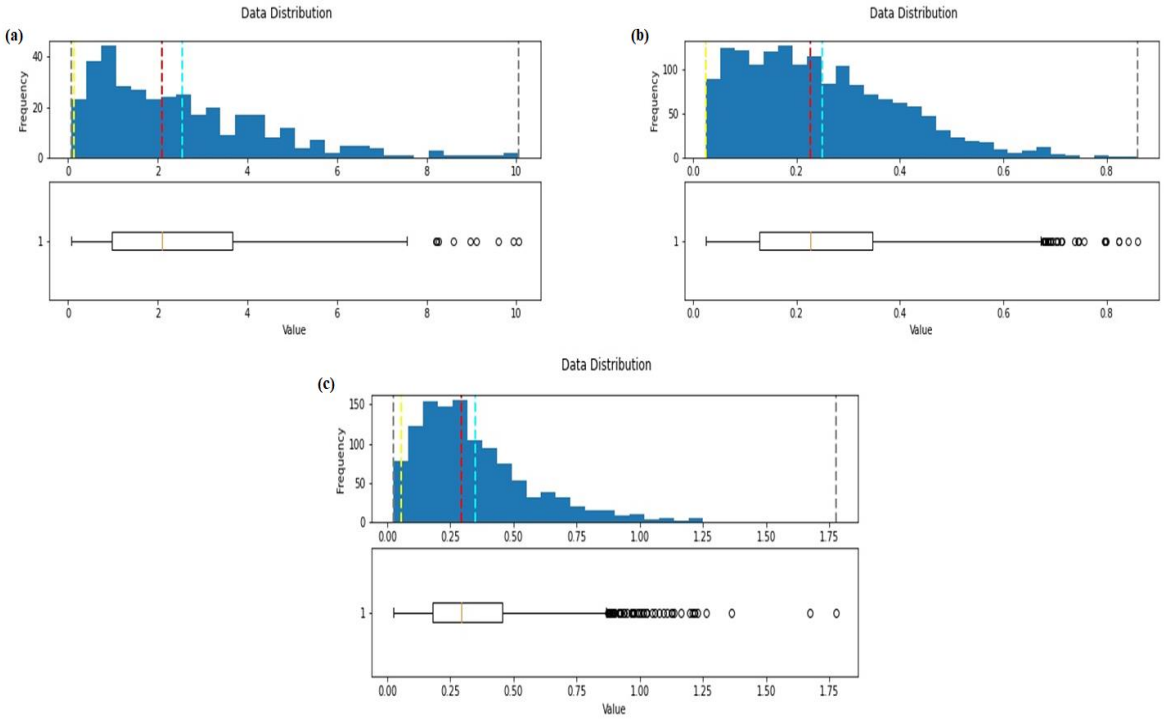

Fig. 11 Distribution of the membranes microstructures with respect to the mean and the radius pore distribution of (a) M1, (b) M2, (c) M3

3.4 Evaluation of membrane performance

The increase in the ratio of GO embedded in the PET membranes induces less water flux and a higher rejection rate (See Figs. 12 and 13). This is in conformity with the data generated from the statistical analysis. The % rejection of the three membranes increase with increase in time. M3 membrane gave higher rejection rate for the three anions and iron. The % rejection of nitrate ion with M3 membrane is 96%, 85%%, 72% and 60% respectively for NO^{3-}, Cl^{-}, HCO^{3-} and Fe. In addition, the high rejection of anions was due to the decrease in the membrane pore size; this is confirmed from the pore sizes obtained from ImageJ studies. However, the low rejections of Fe can be accredited to the decreased concentration of the Fe in the membrane phase. This occurs in electrolyte mixtures due to the acceleration of such ions by the electric field of diffusion potential arising because of strong rejections of other mixture components [36].

Lower flux ensued as a result of aggregation in the course of membrane synthesis which causes reduction in the number of pores (see Fig. 7a). This was also confirmed in Fig. 10, showing tight clustered radius data distribution around the mean. Hence, the lack of aggregation can occur when low probability of the GO particles approaches shorter distances due to the impact spawned by the PET-graphene oxide nanocomposite membranes matrix [37]. Furthermore, PET-graphene oxide nanocomposite membranes with 3wt% GO showed higher porosity,

which is demonstrated in the SEM image and the pore size distribution (see Figs. 5c and 7c); hence, the maximum water flux was attained at 3wt% GO. The further increase in the quantity of GO (2wt% and 3wt%) increased water flux. The transport mechanism responsible for reduction in flux in this study is the pore size of the membranes. The transport description responsible for this mechanism is inserted in Fig. 13. This description shows that pore blockage occurred; hence, the reduction in flux.

The river water was used as the adsorption study. The effect of adsorption in Fig. 14 showed that the adsorption increases with time. The adsorption sites of the membranes three were not all occupied at the initial stage of adsorption (at 20 min) [38]; hence, lower adsorption at that time. The molecules of the anions and iron quickly combined with the adsorption sites as the time increases; thus, the adsorption rate was fast with time. The adsorption capacity of M1 membrane depicts lower capacity than that of M2 and M3 membranes. This is accredited to the increase in the integration of GO in the PET polymer resulting in better adsorption capacity; which aided the accumulation of water film of the membrane. The nitrate, chlorine and iron reached equilibrium at 80 min except for bicarbide.

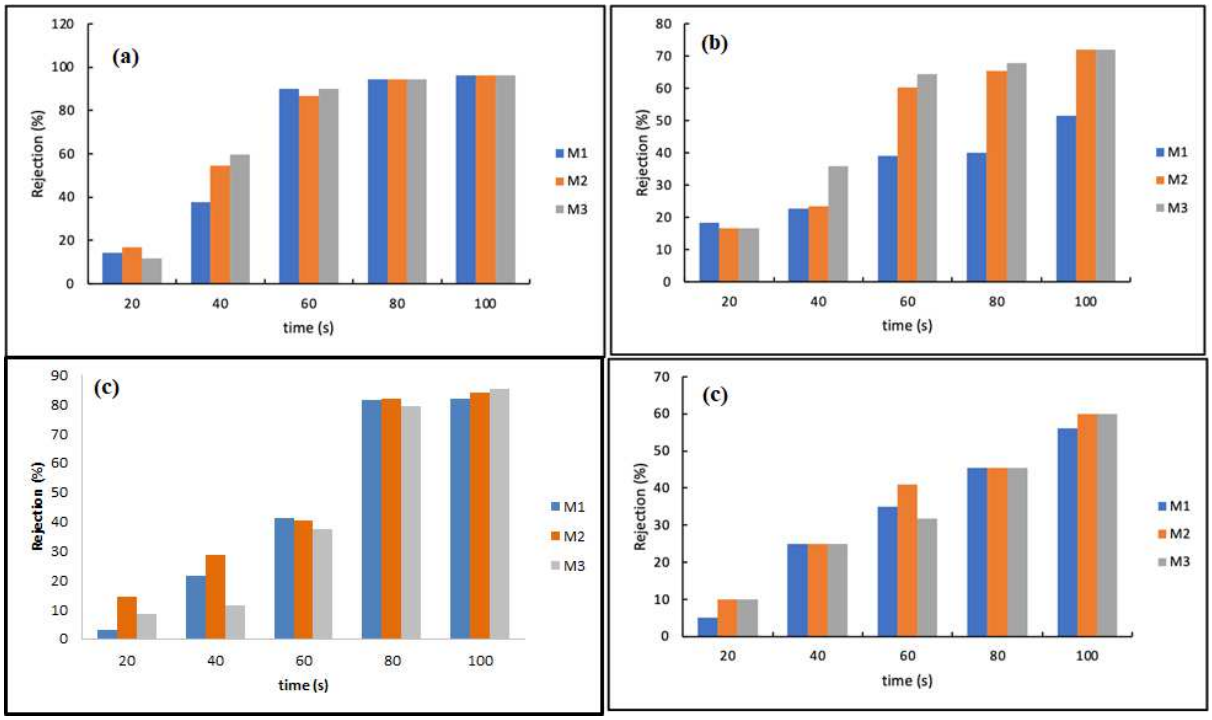

Fig. 12 Rejection of (a) (NO^{3-}) anion, (b) (Cl^{-}) anion, (c) (HCO^{3-}) anion and (d) Fe cation

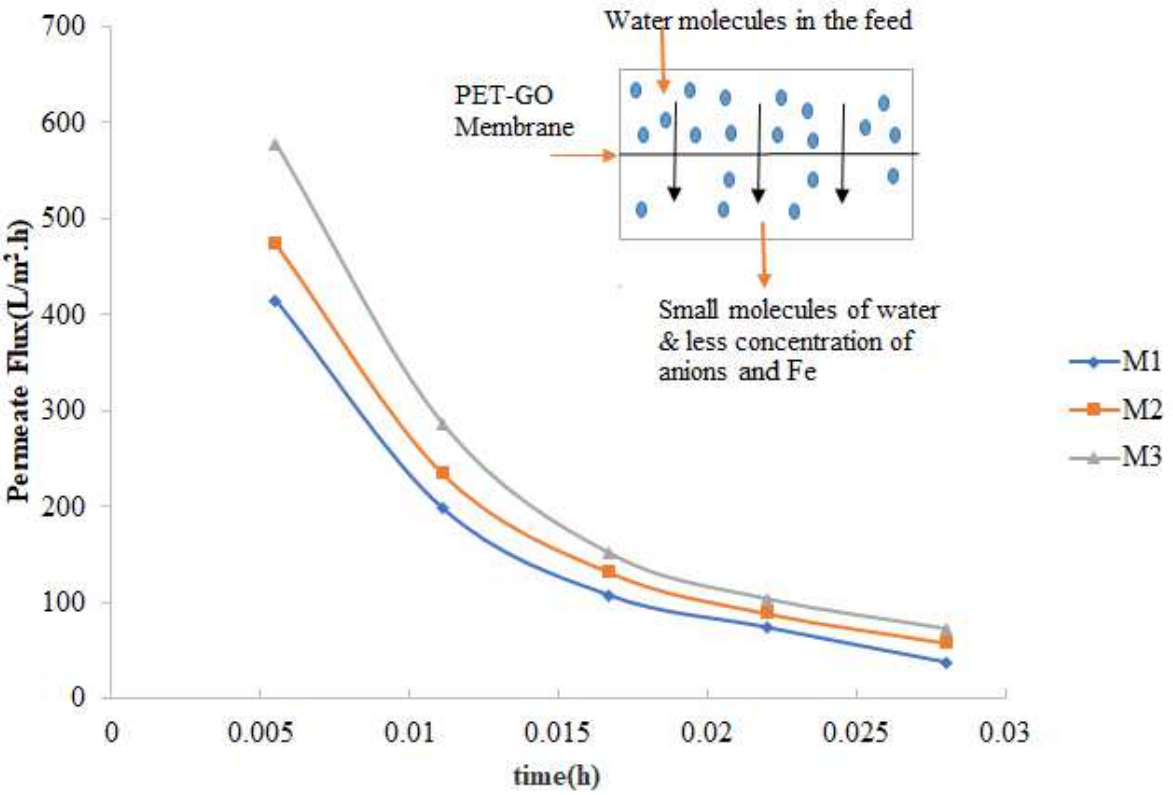

Fig. 13 Normalized flux from the PET-graphene oxide nanocomposite membranes

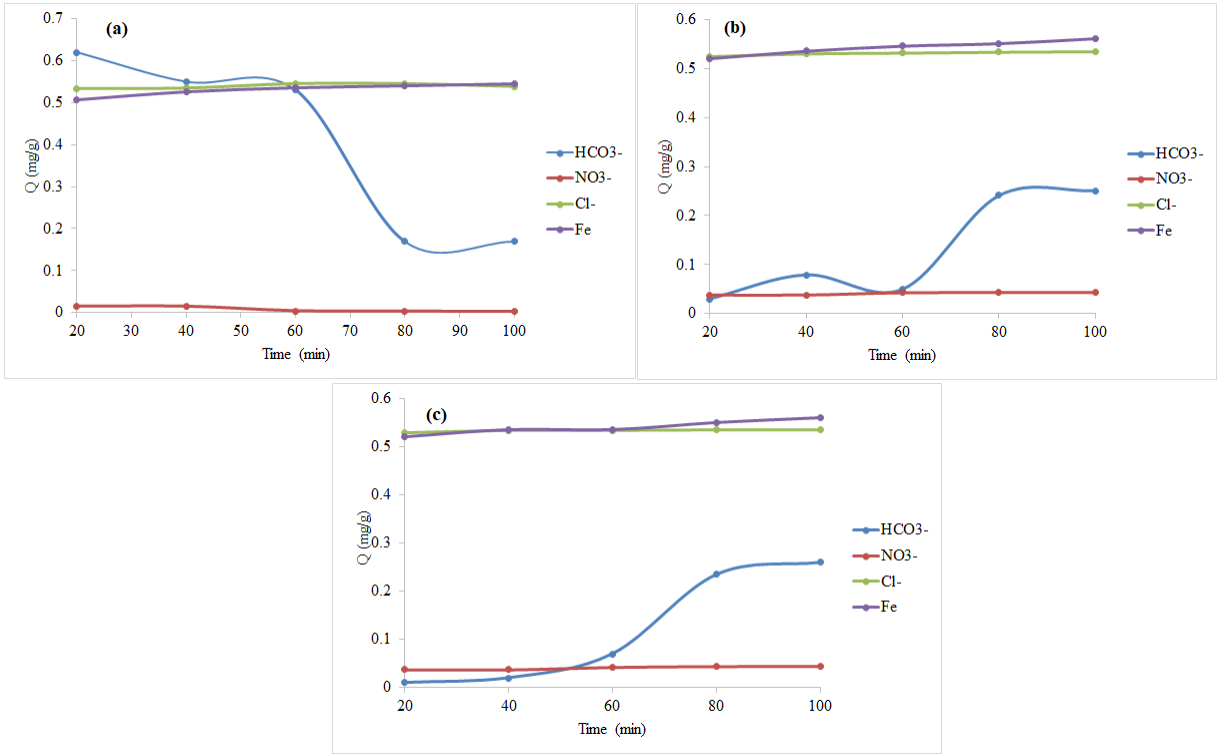

Fig. 14 Effect of the iron and anions adsorption time on adsorption capacity

Conclusion

PET-graphene oxide nanocomposite membranes were fabricated non-solvent-induced phase separation on polyester nonwoven support using PEG as additive. Increasing the amount of GO in the course of fabrication resulted to the reduction in the membrane pore sizes. The effective surface porosity increased with an increase in the quantity of GO embedded in the membrane. The pore size distribution was studied using Image J. The statistical study was done via Gaussian filter distribution by using quartiles analysis. The mean and mode were regarded as the best measure of central tendency as it contains all the features of an ideal microstructure measure. The radius data distribution was tightly clustered around the mean. The composite ratio of GO in PET has impact on the rejection and flux behaviour of the membranes for the removal of iron from Ibese river water. The study has established that the association of PET with GO to make nanocomposites membrane is a promising means in attaining membranes with better performances; as higher rejection rate was attained. In addition, statistical obtained showed that Gaussian distribution using Quartiles analysis is an effective method that relates to the study of permeate flux.

Statement and Declaration

Declaration of Competing Interest

The authors declare that we have no known competing interests with regards to finance and personal relationships that could have appeared to influence the work reported in this paper.

Source of Funding

The authors declare that no funds of grant were received in the course of preparing this manuscript.

Authors Contributions

Dr Oluranti Agboola conceptualize the project and supervised the project

Mr. Ajibola Ademola Khalih carried out the experiments

Dr. Oladokun Olagoke did the statistical study

Dr. Augustine Omoniyi Ayeni reviewed the report

Mr. Frederick Uzokwe Chukwudubem is responsible for the adsorption study

Dr. Olayemi Odunlami interpreted the adsorption study

Dr. Francis Elehinafe interpreted the characterization of materials

Dr. Abdulrazaq Yahaya Discussed the data

Prof. Ojo Sunday Isaac Fayomi Edited the work

Dr. Lucey Moropeng Interpreted the statistical study

Data availability

The data generated in the course of the study will be made available upon request by the corresponding author.

References

1. Bethi, B, Sonawane SH, Bhanvase, BA, Gumfekar SP (2016) Nanomaterials based advanced oxidation processes for wastewater treatment: A review. Chem Engin Process: Process Intensiication 109:178-189
2. Longs Ecowater (2022) What Are the Effects of Iron in Water? https://longsecowater.com/ [Assessed 23rd March 2022]
3. Department of natural resources (2017) Iron in drinking water. https://dnr.wi.gov/files/pdf/pubs/dg/dg0035.pdf [Assessed 24th March 2022]
4. Oluwafemi AM (2018) The Lagos Water Crisis: Any Role for the Private Sector? Urbanet, https://www.urbanet.info/nigeria-lagos-water-crisis/ [Retrieved 19th January 2022] African J Environ Sci Technol 5(8): 608-615.
5. Yang Y, Pignatello JJ, Ma J, Mitch WA (2016) Effect of matrix components on UV/H_2O_2 and UV/ SO_2 advanced oxidation processes for trace organic degradation in reverse osmosis 28 brines from municipal wastewater reuse facilities. Water Res 89:192-200
6. Beita-Sandí W, Karanil T (2017) Removal of both N-nitrosodimethylamine and trihalomethanes precursors in a single treatment using ion exchange resins. Water Res 124:20-28.
7. Carr SA, Liu J, Tesoro AG (2016) Transport and fate of microplastic particles in wastewater treatment plants. Water Rese 91:174-182.
8. Gaouar MY, Benguella B (2016). Efficient and eco-friendly adsorption using low-cost natural sorbents in waste water treatment. Indian J Chem Technol 23(3):204-209.
9. Younas H, Bai H, Shao J, Han Q, Ling Y, He Y (2017) Super-hydrophilic and fouling resistant PVDF ultrafiltration membranes based on a facile prefabricated surface. J Membr Sci 541: 529-540

10. Wu Z, Zhang C, Peng K, Wang Q, Wang Z (2018) Hydrophilic/underwater superoleophobic graphene oxide membrane intercalated by TiO_2 nanotubes for oil/water separation. Front Environ Sci Eng 12:1-10
11. Gu B, Renaud DL, Sanaei P, Kondic L, Cummings LJ (2020) On the influence of pore connectivity on performance of membrane filters
J. Fluid Mech. 902:1-33
12. Luo M, Wen Q, Liu J, Liu H, Jia Z (2011) Fabrication of SPES/Nano-TiO_2 Composite Ultrafiltration Membrane and Its Anti-fouling Mechanism*. Chinese J Chem Eng 19(1): 45-51
13. Zhao S, Wang P, Wang C, Sun X, Zhang L (2012) Thermostable PPESK/TiO_2 nanocomposite ultrafiltration membrane for high temperature condensed water treatment. Desalination 299:35-43.
14. Li X, Li J, Fang X, Bakzhan K, Wang L, Van der Bruggen B (2016) A synergetic analysis method for antifouling behavior investigation on PES ultrafiltration membrane with self-assembled TiO_2 nanoparticles. J Colloid Interface Sci 469:164-176
15. Khalifa RE, Omer AM, Abd Elmageed MH, Mohy Eld MS (2021) Titanium Dioxide/Phosphorous-Functionalized Cellulose Acetate Nanocomposite Membranes for DMFC Applications: Enhancing Properties and Performance. ACS Omega 6(27): 17194-17202
16. Zinadini S, Zinatizadeh AA, Rahimi M, Vantapour V, Zangene H (2014) Preparation of a novel antifouling mixed matrix PES membrane by embedding graphene oxide nanoplates. J Membr Sci 453:292-301
17. Huang K, Liu G, Lou Y, Dong Z, Shen J, Jin W (2014) A Graphene Oxide Membrane with Highly Selective Molecular Separation of Aqueous Organic Solution. Angewandte Chemie 53(27): 6929-6932
18. Li Y-Y, Gurkan B (2021) Graphene oxide reinforced facilitated transport membrane with poly(ionic liquid) and ionic liquid carriers for CO_2/N_2 separation. J Membr Sci 638: 119652.
19. Tran BN. Thickett SC, Agarwal V, Zetterlund PB (2021) Influence of Polymer Matrix on Polymer/Graphene Oxide Nanocomposite Intrinsic Properties. Appl Polym Mater 3(10): 5145-5154

20. Sali S, Mackey HR, Abdala AA (2019) Effect of graphene oxide synthesis method on properties and performance of polysulfone-graphene oxide mixed matrix membranes. Nanomater 9(769): 1-16
21. Goh PS, Othman MHD, Matsuura T (2021) Waste reutilization in polymeric membrane fabrication: A new direction in membranes for separation. Membr 11:782.
22. Patel SH, Xanthos M (2001) Environmental Issues in Polymer Processing: A Review on Volatile Emissions and Material/Energy Recovery Options; Springer: Berlin/Heidelberg, Germany, 2001; Volume 20.
23. Mansoori S, Davarnejad R, Matsuura T, Ismail AF (2020) Membranes based on non-synthetic (natural) polymers for wastewater treatment. Polym Test 84:106381.
24. Paulchamy B, Arthi G, Lignesh BD (2015). A Simple Approach to Stepwise Synthesis of Graphene Oxide Nanomaterial. J Nanomed Nanotechnol 6(1): 1-4
25. Dunning H (2020) Size determines how nanoparticles affect biological membranes. Imperial College, London. https://www.imperial.ac.uk/news/204433/size-determines-nanoparticles-affect-biological-membranes/#:~:text=They%20found%20that%20larger%20nanoparticles,distorted%20the%20membrane%2C%20bending%20it [Retrieved 24th January 2022]
26. Pulido BA, Habboub OS, Aristizabal SL, Szekely AG, Nunes SP (2019) Recycled Poly(ethylene terephthalate) for High Temperature Solvent Resistant Membranes. ACS Appl Polym Mater 1(9): 2379-2387
27. Diaz-Reinoso B (2020) Chapter 14 - Concentration and purification of seaweed extracts using membrane technologies. In: Sustainable seaweed technologies. p. 371-390
28. De Meis D (2017) Overview on Porous Inorganic Membranes for Gas Separation. RT/2017/5/ENEA. (Retrieved 25th January 2022)
29. Agboola O, Maree J, Mbaya R (2014) Characterization and performance of nanofiltration membranes. Environ Chem Lett 12:241-255
30. Altschuh P, Yabansu YC, Hötzer J, Selzer M, Nestler B, Kalidindi SR (2017) Data science approaches for microstructure quantification and feature identification in porous membranes. J. Membr Sci 540:88-97
31. Nethravathi C, Rajamathi CR, Rajamathi M, Wang X, Gautam UK, Golberg D, Bando Y (2014) Cobalt hydroxide/oxide hexagonal ring-graphene hybrids through chemical

etching of metal hydroxide platelets by graphene oxide: Energy storage applications. ACS Nano 8:2755-2765

32. Paranthaman V, Sundaramoorthy K, Chandra B, Pandian S, Alagarsamy MP, Perumalsamy R (2018) Investigation on the Performance of Reduced Graphene Oxide as Counter Electrode in Dye Sensitized Solar Cell Applications. Phys Status Solidi A 215:1-9
33. Nguyen HTV, Ngo THA, Do KD, Nguyen MN, Dang NTT, Nguyen TTH, Vien V, Vu TA (2019) Preparation and Characterization of a Hydrophilic Polysulfone Membrane Using Graphene Oxide. J Chem 1-11
34. Jang J, Park I, Chee S-S, Song J-H, Kang Y, Lee C, Lee W, Ham M-H, Kim IS (2020) Graphene oxide nanocomposite membrane cooperatively cross-linked by monomer and polymer overcoming the trade-off between flux and rejection in forward osmosis. J Membr Sci 598: 117684
35. Suntornnond R, An J, Tijore A, Leang KF, Chua CK, Tan LP (2016) A Solvent-Free Surface Suspension Melt Technique for Making Biodegradable PCL Membrane Scaffolds for Tissue Engineering Applications. Molecules 21(386): 1-13
36. Yaroshchuk AE (2008) Negative rejection of ions in pressure-driven membrane processes. Adv Colloid Interface Sci 139:150-173
37. Dukhin AS, Goetz PJ (2017) Characterization of liquids, dispersions, emulsions and porous materials using ultrasound. 33r Edition, Elsevier
38. Tang Q, Li N, Lu Q, Wang X, Zhu Y (2019) Study on Preparation and Separation and Adsorption Performance of Knitted Tube Composite-Cyclodextrin/Chitosan Porous Membrane. Polym 11:1-17